PERGAMON

Chemical Engineering Science 54 (1999) 5013–5019

Chemical Engineering Science

Multicomponent reaction engineering model for Fe-catalyzed Fischer–Tropsch synthesis in commercial scale slurry bubble column reactors

Gerard P. van der Laan[a], Antonie A.C.M. Beenackers[a,*], Rajamani Krishna[b]

[a]*University of Groningen, Department of Chemical Engineering, Nijenborgh 4, 9747 AG Groningen, The Netherlands*
[b]*University of Amsterdam, Department of Chemical Engineering, Nieuwe Achtergracht 166, 1018 WV Amsterdam, The Netherlands*

Abstract

A multicomponent mathematical model is presented for a large-scale slurry bubble column reactor operating in the heterogeneous or churn-turbulent flow regime. The model accounts for both the Fischer–Tropsch reaction as well as the water gas shift reaction and the individual paraffin and olefin formation rates. It provides all the data necessary for reliable scale up, process optimization and prediction of the performance of industrial scale Fischer–Tropsch bubble column reactors.

Keywords: Fischer-Tropsch reactor design; Bubble column; Slurry reactor; Iron catalyst; Modeling

1. Introduction

Synthesis gas (CO and H_2) from coal or natural gas can be converted in the Fischer–Tropsch (FT) process to a multicomponent mixture of predominantly linear hydrocarbons. The FT synthesis in slurry bubble column reactors (SBCR) is very attractive relative to fixed-bed reactors (Saxena, Rosen, Smith & Ruether, 1986) Mathematical modeling of a FT SBCR was reviewed by Saxena et al. (1986). The bottle neck appears to be the lack of reliable kinetic equations for all products and reactants based on realistic reaction mechanisms. Until now, none of the available literature models can describe the complete product distribution of the FT synthesis at industrial conditions (high temperature and pressure) as a function of overall consumption of synthesis gas components and operating conditions. Furthermore, most hydrodynamic models published in literature are only applicable to small-scale bubble columns operating in the homogeneous regime. However, the churn-turbulent or heterogeneous flow regime is the most optimal one for the FT synthesis (De Swart, Krishna & Sie, 1997). Krishna and co-workers modeled an SBCR containing cobalt catalyst particles with the use of flow patterns for the large and small gas bubbles (De Swart et al., 1997; Krishna & Maretto, 1998). This study will investigate an iron-based Fischer–Tropsch SBCR operating in the heterogeneous flow regime. The model takes into account both the water gas shift (WGS) and the FT reactions, as well as individual hydrocarbon product formation rates. Here, multicomponent vapor–liquid equilibria (VLE) with detailed kinetic expressions for all reactants and hydrocarbon products are combined with SBCR hydrodynamics and mass transfer characteristics to predict the detailed product composition of both the gas and liquid phase as a function of operating conditions.

2. Kinetics and hydrocarbon selectivity

The Fischer–Tropsch process is a combination of the FT and WGS reactions:

$$\mathrm{CO} + (1 + m/2n)\mathrm{H_2} \rightarrow 1/n\mathrm{C}_n\mathrm{H}_m + \mathrm{H_2O} \quad (R_{FT}, -\Delta H_{FT} = 165\ \mathrm{kJ\ mol^{-1}}), \tag{1}$$

$$\mathrm{CO} + \mathrm{H_2O} \rightleftarrows \mathrm{CO_2} + \mathrm{H_2} \quad (R_{\mathrm{WGS}}, -\Delta H_{\mathrm{WGS}} = 41\ \mathrm{kJ\ mol^{-1}}) \tag{2}$$

* Corresponding author. Tel.: +31-50-3634484; fax: +31-50-3634479.

E-mail address: a.a.c.m.beenackers@chem.rug.nl (A.A.C.M. Beenackers)

0009-2509/99/$ - see front matter
PII: S0009-2509(99)00225-0

Nomenclature

a_c	specific cooling area, m^{-1}
A	reactor area, m^2
C	concentration, mol m^{-3}
C_p	heat capacity, J kg^{-1} K^{-1}
D	reactor diameter, m
D	diffusion coefficient, m^2 s^{-1}
F	H_2/CO feed ratio
h	axial position, m
H	dispersion height, m
H_i^{∞}	Henry constant, Pa
k_La	volumetric mass transfer coefficient, s^{-1}
K_i	equilibrium constant (y_i/x_i)
m_i^{GL}	solubility coefficient C_G/C_L
m_i	molar selectivity
P	pressure, Pa
P_i^{sat}	vapor pressure, Pa
R	gas constant, 8.314 J mol^{-1} K^{-1}
R_j	reaction rate, mol kg_{cat}^{-1} s^{-1}
T	temperature, K
U	H_2/CO consumption ratio ($-R_{H_2}/-R_{CO}$)
U	superficial velocity, m s^{-1}
V_R	reactor volume, m^3
V_{small}	rise velocity small bubbles, m s^{-1}
w_i	weight fraction of product i
X_{CO+H_2}	synthesis gas conversion
X_{H_2}	hydrogen conversion
x_i	mole fraction in liquid phase
y_i	mole fraction in gas phase

Greek letters

α_{eff}	effective heat transfer coefficient, W m^{-2} K^{-1}
α_c	contraction factor
γ_i^{∞}	liquid phase activity coefficient
$\Delta H_{R,j}$	reaction enthaphy, J mol^{-1}
ε	holdup
η_L	liquid viscosity, Pa s
v_{ij}	stoichiometric coefficient
ρ	density, kg m^{-3}
σ	surface tension, N m^{-1}
Φ_i	Poynting factor
$\Phi_{v,0}/W$	space velocity, Nm^3 kg_{cat}^{-1} s^{-1}

Sub- and Superscripts

B	large bubbles
c	coolant
DF	dense phase
G	gas phase
i	component
in	inlet conditions
j	reaction
L	liquid phase
large	referring to large bubbles
out	outlet conditions
P	catalyst phase
R	reactor
ref	reference conditions
S	slurry phase
small	referring to small bubbles
$a, b, k, K_P, k_{WGS}, K, t_P^1, t_P^2, k_R^2, p, t_O, k_R, c, \alpha_n, \theta_n$	Kinetic and selectivity parameters (See Section 2):

where n is the average carbon number and m is the average number of hydrogen atoms of the hydrocarbon products. Both n and m vary with catalyst type and reaction conditions. The rate expression for the FT reaction on a precipitated iron catalyst in the slurry phase proposed by Van der Laan (1999) was used (Eq. (3), Table 1). The water gas shift reaction is an exothermic and reversible reaction proceeding simultaneously with the Fischer–Tropsch reaction. Due to the WGS reaction, synthesis gas with a H_2/CO ratio below 2 can be used because excess of carbon monoxide is converted with water to carbon dioxide and hydrogen. The equilibrium constant K_P was obtained from Graaf, Sijtsema, Stamhuis and Joosten (1986) and the following rate expression was used for the kinetics of the WGS (Van der Laan, 1999) (see Table 1):

$$R_{WGS} = \frac{k_{WGS}(P_{CO}P_{H_2O} - P_{CO_2}P_{H_2}/K_P)}{(P_{CO} + KP_{H_2O})^2},$$

$$R_{FT} = \frac{kP_{CO}P_{H_2}^{1/2}}{(1 + aP_{CO} + bP_{CO_2})^2}. \quad (3)$$

The product selectivity to α-olefins and paraffins was calculated using a recently developed selectivity model for iron catalysts, called α-olefin readsorption product distribution model (ORPDM) (Van der Laan, 1999; Van der Laan & Beenackers, 1998). This model allows for a chain-length-dependent chain growth factor due to readsorption of α-olefins.

$$\frac{\theta_n}{\theta_{n-1}} = \frac{p}{t_O/(1 + k_R e^{cn}) + 1 + p} = \alpha_n,$$

$$\frac{\theta_2}{\theta_1} = \frac{p}{t_O^2/(1 + k_R^2) + t_P^2 + p} = \alpha_2. \quad (4)$$

Table 1
Kinetic and selectivity model parameters at 523 K (Van der Laan, 1999)

Parameter	Value	Parameter	Value
t_P^1	6.5 ($m_{CH_4} = t_P^1\theta_1$)	k (mol kg^{-1} s^{-1} MPa$^{-1.5}$)	0.0339
t_P^2	1.7 ($m_{C_2H_6} = t_P^2\alpha_2\theta_1$)	a (MPa^{-1})	1.185
c	0.35	b (MPa^{-1})	0.656
k_R^2	17.6 $k_R e^{2c}$($m_{C_2H_4} = t_P^2 t_O \alpha_2\theta_1/(1 + k_R^2)$)	k_{WGS} (mol kg^{-1} s^{-1})	0.0292
p	14.0 $P_{H_2}^{-0.26}P_{CO}^{0.40}$	K (dimensionless)	3.07
t_O	3.71 $P_{H_2}^{-0.5}$	K_P	85.81
k_R	8.00×10^{-5} $P_{H_2}^{1.2}P_{CO}^{-0.47}/\Phi_{v,0}/W$		

Pressures in MPa, space velocity $\Phi_{v,0}/W$ in Nm^3 kg$_{cat}^{-1}$ s^{-1}

The product selectivities to paraffins and olefins follow from:

$$m_{C_nH_{2n+2}} = \theta_1 \prod_{i=2}^{n} \alpha_i, \quad m_{C_nH_{2n}} = \frac{t_O}{1 + k_R e^{cn}} \theta_1 \prod_{i=2}^{n} \alpha_i,$$

$$\sum_{i=1}^{\infty} m_i = 1. \tag{5}$$

The molar selectivities of the C_1 and C_2 products are calculated differently (Van der Laan & Beenackers, 1998) (see Table 1). The appropriate model parameters are shown in Table 1 as a function of process variables (P_{CO}, P_{H_2}, $\Phi_{v,0}/W$) at a constant temperature of 523 K.

3. Model equations

A mathematical description for the simulation of an industrial Fischer–Tropsch SBCR is presented. The reactor model can be applied in the heterogeneous or churn-turbulent regime (see Fig. 1). The large bubbles are assumed to be in plug flow with a superficial gas velocity of $U_G - U_{DF}$. The superficial velocity of the gas present in the well-mixed small bubbles is U_{DF}, which is equal to the total superficial gas velocity at regime transition. The mathematical model for the Fischer–Tropsch synthesis is based on the following assumptions: (1) Gas–liquid mass transfer resistance is located in the liquid phase. (2) Large gas bubbles are in plug flow due to high rise velocities, typically 1–2 m s^{-1}. (3) The gas phase in the small gas bubbles, and the liquid phase are each completely mixed, due to the large reactor diameter of 8 m (Deckwer, Serpeman, Ralek & Schmidt, 1982). Catalyst distribution is uniform due to upflow of the slurry phase, the large reactor diameter and the turbulence created by the fast-rising large bubbles. (4) Hydrocarbon products, paraffins and olefins only, in the gas and liquid phase of the reactor outlet are assumed to be in equilibrium at the reactor outlet. (5) The reactor operates isothermally due to the completely mixed liquid phase. (6) The slurry velocity is constant. (7) The reactor operates at steady state conditions. (8) The effectiveness factor of the catalyst particles is equal to unity and mass and heat transfer resistances between catalyst and liquid are negligible due to the small particle size applied (50 μm).

The gas-phase mass balance for component i in the large bubbles, rising in plug flow is

$$\frac{\mathrm{d}(U_G - U_{DF})C_{i,G}^{\text{large}}}{\mathrm{d}h} + (k_L a)_i^{\text{large}}\left(\frac{C_{i,G}^{\text{large}}}{m_i^{GL}} - C_{i,L}\right) = 0 \tag{6}$$

with concentrations in mol m^{-3} subject to the boundary conditions at the reactor entrance: $h = 0$: $C_{i,G}^{\text{large}} = C_{i,G}^{\text{in}}$. The gas-phase mass balance for component i in the *small* bubbles (completely mixed) is

$$\frac{U_{DF}}{H}(C_{i,G}^{\text{in}} - C_{i,G}^{\text{small}}) = (k_L a)_i^{\text{small}}\left(\frac{C_{i,G}^{\text{small}}}{m_i^{GL}} - C_{i,L}\right). \tag{7}$$

The mass balance for component i in the completely mixed liquid phase can be written as

$$1/H\int_0^H (k_L a)_i^{\text{large}}\left(\frac{C_{i,G}^{\text{large}}}{m_i^{GL}} - C_{i}{,}L\right)\mathrm{d}h + (k_L a)_i^{\text{small}}\left(\frac{C_{i,G}^{\text{small}}}{m_i^{GL}} - C_{i}{,}L\right) + \varepsilon_L\varepsilon_P\rho_P\sum_{j=1}^{n} v_{ij}R_j - \frac{U_S}{H}C_{i,L} = 0, \tag{8}$$

where ε_L is the liquid holdup ($m_L^3\, m_R^{-3}$), ε_P is the solids holdup $m_P^3\, m_L^{-3}$, ρ_P is the catalyst density, R_j is the FT ($j = 1$) or WGS ($j = 2$) reaction rate (mol kg$_{cat}^{-1}$ s^{-1}), v_{ij} is the stoichiometric coefficient for component i in the jth reaction. The reaction heat is removed with vertical cooling tubes of 1.5 inch diameter at a constant steam temperature T_c of 495 K. The overall heat transfer coefficient α_{eff} from slurry to coolant is estimated from the correlation of Deckwer et al. (1982). The energy balance for the slurry phase reads, assuming that catalyst and the liquid temperature are equal

$$\varepsilon_L\varepsilon_P\rho_P\sum_{j=1}^{n}(-\Delta H_{R,j})R_j - \alpha_{\text{eff}}a_c(T - T_c) + \frac{U_S}{H}((\rho_S C_{p,S}T)_{\text{in}} - (\rho_S C_{p,S}T)_{\text{out}}) = 0, \tag{9}$$

where a_c is the specific heat transfer area (m^{-1}), $C_{p,S}$ is the heat capacity of the slurry phase, ρ_S is the slurry density and $-\Delta H_{R,j}$ is the reaction heat of reaction j (J mol^{-1}).

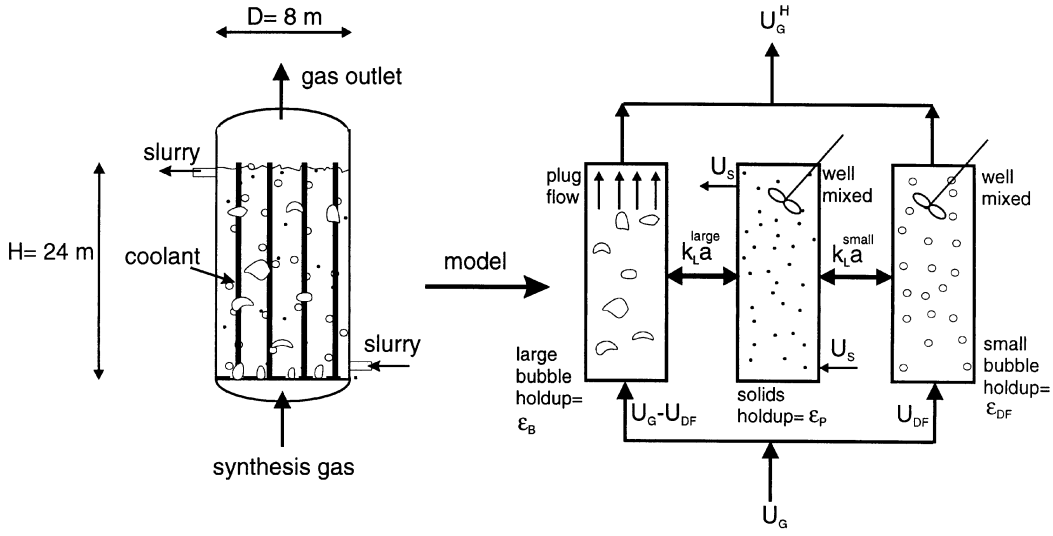

Fig. 1. Hydrodynamic model of slurry bubble column reactor in the heterogeneous flow regime

The molar flow rate of the gas phase will change due to reaction. The superficial velocity is assumed to be a linear function of the overall synthesis gas conversion, X_{CO+H_2} (Mills, Turner, Ramachandran & Dudukovic, 1996)

$$U_G = (1 + \alpha_c X_{CO+H_2})U_G^{in} = (1 + \alpha_c(1 + U)/(1 + F)X_{H_2})U_G^{in},$$

where α_c is the contraction factor, U is the usage ratio of hydrogen to carbon monoxide ($-R_{H_2}/-R_{CO}$) and F is the feed ratio of H_2 to CO. The reported values of α_c are between -0.5 and -0.65 (Van der Laan, 1999; Deckwer et al., 1982). The contraction factor α_c is determined by the product selectivity (m and n, see Eq. (1)).

4. Hydrodynamic parameters

The most important hydrodynamic parameters are the gas holdup of the large and small bubbles in presence of solids under Fischer–Tropsch reaction conditions. The rise velocity of the small bubbles will increase with increasing solids holdup due to enhanced coalescence according to

$$V_{small} = V_{small}^{ref}(1 + 0.8\varepsilon_P/V_{small}^{ref})$$

with $V_{small}^{ref} = 0.095\ m\ s^{-1}$ (Krishna, De Swart, Ellenberger, Martina & Maretto, 1997). The gas holdup at the transition from homogeneous to churn turbulent regime in the presence of a high solids loading follows from Krishna et al. (1997):

$$\varepsilon_{DF} = \varepsilon_{DF}^{ref}(\rho_G/\rho_G^{ref})^{0.48}(1 - 0.7\varepsilon_P/\varepsilon_{DF}^{ref}), \quad (10)$$

where the small bubble holdup in solids-free liquid is $\varepsilon_{DF}^{ref} = 0.27$ and the atmospheric density is $\rho_G^{ref} = 1.3\ kg\ m^{-3}$. The corresponding superficial gas velocity at regime transition is calculated from $U_{DF} = V_{small}\varepsilon_{DF}$. The model of Krishna and Ellenberger (1996) is used to predict the gas holdup of the *large* bubbles. This model is corrected for the influence of gas density according to a recent study of Letzel, Schouten, Krishna and Van den Bleek (1999). For large bubble columns ($D > 1$ m) and high slurry concentrations ($\varepsilon_P > 0.16$), the large bubble holdup can be estimated from a combination of the correlations given by Letzel et al. (1999) and Krishna et al. (1997):

$$\varepsilon_B = 0.3(U_G - U_{DF})^{0.58}(\rho_G/\rho_G^{ref})^{0.5}. \quad (11)$$

The total gas holdup in the heterogeneous regime is calculated from: $\varepsilon_G = \varepsilon_B + \varepsilon_{DF}(1 - \varepsilon_B)$. The volumetric mass transfer coefficient of large bubbles is obtained from the relation proposed by Vermeer and Krishna (1981) and more recently by Letzel et al. (1999): $k_L a_{ref}^{large}/\varepsilon_B = 0.5$, which is corrected for the mass transfer coefficient of component i by the factor $k_{L,i}^{large}/k_{L,ref}^{large} = (D_i/D_{ref})^{0.5}$ where $D_{ref} = 2 \times 10^{-9}\ m^2\ s^{-1}$. In the same way, the volumetric mass transfer coefficient for component i of the small bubbles is defined as: $k_L a_{ref}^{small}/\varepsilon_{DF} = 1.0$ (Krishna & Maretto, 1998).

5. Physical properties and flash calculations

For calculating the physical properties of the liquid, it was assumed that the FT wax consisted of *n*-paraffins with a carbon number of 28 ($C_{28}H_{58}$). The asymptotical behavior correlations developed by Marano and Holder (1997b,c) then give at 523 K: surface tension $\sigma = 0.017\ N\ m^{-1}$, liquid density $\rho_L = 656.7\ kg\ m^{-3}$, liquid viscosity $\eta_L = 5.95 \times 10^{-4}$ Pa s, and heat capacity

$C_{p,L} = 2721\ \mathrm{J\,kg^{-1}\,K^{-1}}$. Henry constants for CO, CO_2, H_2, H_2O, N_2 and light hydrocarbons (C_1–C_3) were obtained from Marano and Holder (1997a). Diffusivities at high temperatures and pressures, necessary for calculating mass transfer coefficients, were estimated using correlations of Erkey, Rodden and Akgerman (1990) based on the rough hard sphere theory. The multicomponent VLE model of Marano and Holder (1997a) was applied. However, we assumed ideal gas behavior of the gas phase because under the reaction conditions applied, the fugacity coefficients (up to C_{30}) as calculated with the Peng–Robinson equation of state are between 0.95 and 1.01. The equilibrium constants between vapor and liquid for non-hydrocarbons and C_{1-3} hydrocarbons were calculated from: $K_i \equiv y_i/x_i = H_i^{\infty}\Phi_i/P$, where H_i^{∞} is the Henry constant for component i at infinite dilution, and Φ_i is the Poynting factor. For the other hydrocarbons, the K-value is given by: $K_i = \gamma_i^{\infty} P_{i,\mathrm{sat}}\Phi_i/P$ where γ_i^{∞} is an activity coefficient, and $P_{i,\mathrm{sat}}$ is the vapor pressure of the pure component i. The appropriate parameter values were obtained from Marano and Holder (1997a). A flash calculation using these K-values gives the final composition of the liquid- and gas-phase outlet of the SBCR: $\rho_p \bar{\varepsilon}_L \varepsilon_P V_R R_{FT} m_i/(\sum m_i n) = U_G^H A y_i C_G + U_S A x_i C_L$, where m_i is the molar selectivity to product i with carbon number n, and C_G and C_L are the total gas and liquid concentrations, respectively.

6. Results and discussion

A commercial scale SBCR with diameter $D = 8$ m, dispersion height $H = 24$ m, pressure $P = 3.0$ MPa and temperature $T = 523$ K is used in our simulations. The superficial slurry velocity U_S is $0.01\ \mathrm{m\,s^{-1}}$. The slurry enters the reactor with an inlet temperature of 423 K. The properties of the catalyst applied (Ruhrchemie LP 33/81 Fe/Cu/K on SiO_2) are: catalyst particle diameter 50×10^{-6} m, catalyst density $\rho_P = 1957\ \mathrm{kg\,m^{-3}}$. The properties of the slurry were determined using the relations of Deckwer et al. (1982). The complete reactor model consists of a system of ordinary differential equations and algebraic equations, with the corresponding boundary conditions. The set of equations was solved numerically using a backward differentiation scheme with 60 grid points using the gPROMS software package (Version 1.6a, Process Systems Enterprise, London). The concentration gradients of CO, H_2, CO_2, H_2O and N_2 are large in the bottom of the slurry reactor. Particularly at the top of the reactor, the liquid phase is in equilibrium with the gas phase ($C_{i,L} = C_{i,G}^{\mathrm{large}}/m_i^{GL}$). Resulting from the difference in solubility, the H_2/CO ratio in the liquid-phase is larger than that in the gas feed. The liquid-phase concentrations of H_2 and CO influence the chain length and olefin content of the products formed. Fig. 2 shows the corresponding productivity of each

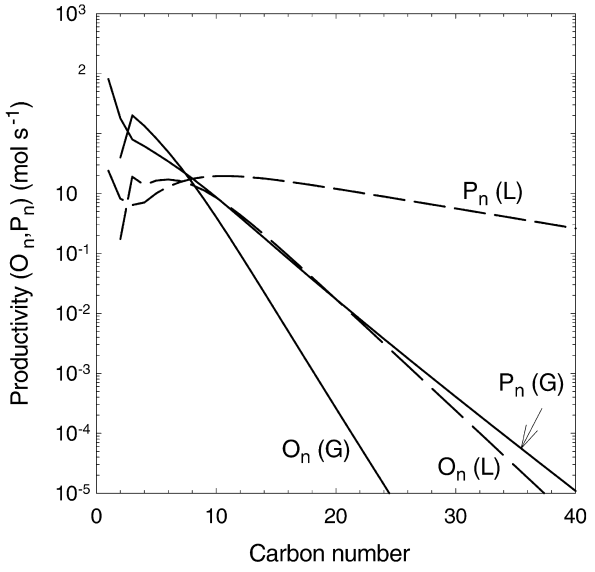

Fig. 2. Paraffin (P_n) and olefin (O_n) production rates in the gas and liquid outlet streams ($p = 12.6$, $t_O = 4.6$, $k_R = 0.27$). Operating conditions: $F = 1$, $U_G^{\mathrm{in}} = 0.20\ \mathrm{m\,s^{-1}}$, $\varepsilon_P = 0.25$, $D = 8$ m, $H = 24$ m, $T = 523$ K.

individual paraffin and olefin, both in the gas and liquid phase. The model predicts the FT product distribution between the vapor and liquid phases. The lighter products with a high olefin yield are in the gas phase, and the heavier products, mainly paraffins, leave the reactor in the liquid or wax phase. Our model predicts the effect of the process conditions on the selectivity and composition of the individual phases.

The major results of our simulations on the reactor performance are shown in Fig. 3a and b for a range of catalyst concentrations ε_P between 0.2 and 0.35, feed ratios of H_2 to CO (F) in the synthesis gas between 0.67 and 2, with a constant mole fraction of CO_2 and N_2 in the feed of 0.05 and superficial inlet gas velocity U_G^{in} from 0.15 to 0.4 m s^{-1}. Increase of the inlet gas velocity causes a decrease of the synthesis gas conversion, as expected. At low gas velocities, $U_G^{\mathrm{in}} < 0.15\ \mathrm{m\,s^{-1}}$, the synthesis gas conversion reaches a constant level of about 80% as a consequence of the kinetic expressions with product (CO_2) inhibition. Higher conversions can be obtained when the operating conditions (P, T) or catalyst are changed or when the dispersion height is increased to, for example, $H = 30$ m. The reactor productivity, expressed as total hydrocarbon production in $\mathrm{kg\,h^{-1}\,m_R^{-3}}$, shows an increase with increasing gas velocity. The effect of catalyst concentration on the reactor performance at $F = 1$ is shown in Fig. 3a. Increasing the catalyst concentration (ε_P) shows an increase of the conversion and productivity. The catalyst concentration influences the concentration levels as well as ε_{DF} according to Eq. (10). The highest productivity is obtained at high catalyst concentrations ($\varepsilon_P = 0.35$) and gas velocities up to

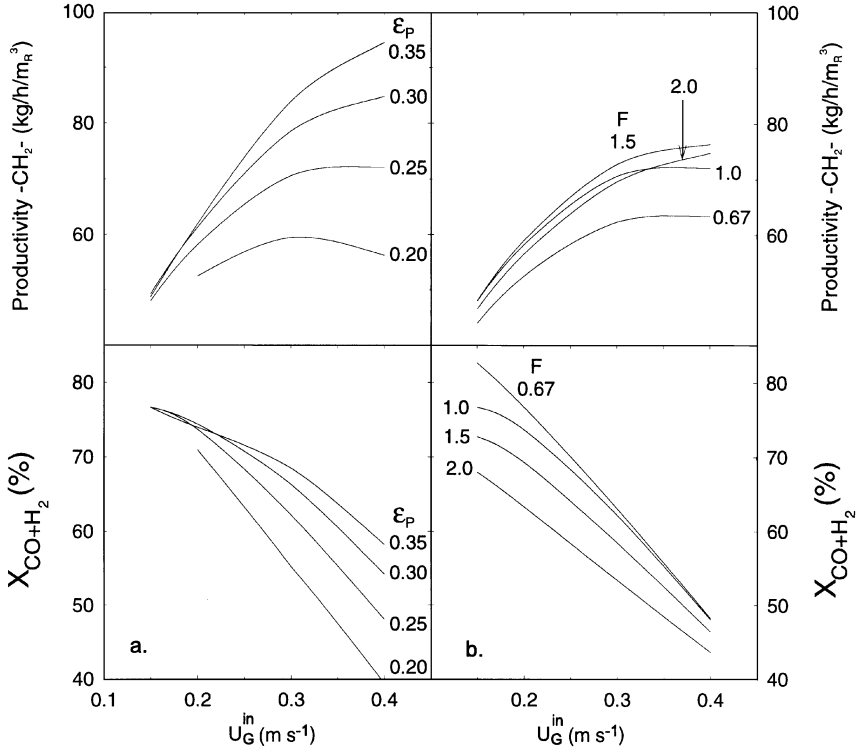

Fig. 3. a. Effect of catalyst concentration and gas velocity on the synthesis gas conversion and productivity ($F = 1$, $T = 523$ K). b. Effect of the H_2/CO feed ratio F and gas velocity on the same ($\varepsilon_P = 0.25$, $T = 523$ K).

Table 2
Selectivity parameters and product selectivities (wt%) as a function of the H_2/CO feed ratio $F(U_G^{in} = 0.20\ m\ s^{-1}$, $\varepsilon_P = 0.25$, $T = 523$ K)

				Product selectivity (wt%)						
F	p	t_O	k_R	w_1	w_{2-4}	w_{5-10}	w_{10+}	$w_{O,2}$	$w_{O,3-4}$	w_O
0.67	17.4	5.6	0.17	3.7	17.5	26.5	52.3	43.0	85.3	37.7
1.0	12.6	4.6	0.27	5.7	18.9	27.2	48.2	28.5	79.3	33.5
1.5	9.6	3.9	0.41	8.2	20.5	28.4	43.0	19.0	72.7	29.6
2.0	7.9	3.6	0.56	10.6	21.8	29.3	38.3	13.9	66.8	26.5

0.4 m s^{-1}. The effect of the feed ratio F at a constant catalyst concentration of $\varepsilon_P = 0.25$ is given in Fig. 3b. The decrease of the synthesis gas conversion with increasing F is mainly caused by the kinetics. At low feed ratios, conversions of CO are large due to the high water gas shift reaction rate. The optimal productivity is obtained at a feed ratio of $F = 1.5$. The feed ratio influences the gas holdup due to changing gas density. Significantly lower gas holdup values were observed with increasing F. The number of cooling tubes required strongly depends on the productivity and varies between 600 and 1700 cooling tubes. The corresponding pitch distance varies from 0.33 to 0.20 m, which is large enough not to influence the hydrodynamics of the SBCR (Krishna & Maretto, 1998).

The effect of the feed ratio on the selectivity to several product classes is shown in Table 2. The total hydrocarbon (paraffin and olefin) selectivities in mass percentages were lumped in to four groups: methane (w_1), light gases C_{2-4} (w_{2-4}), gasoline C_{5-10} (w_{5-10}), and a diesel/wax fraction C_{10-100} (w_{10+}). The olefin content is shown for the C_2 products ($w_{O,2}$), C_{3-4} products ($w_{O,3-4}$) and the total olefin yield of all products (w_O). The selectivities in Table 2 were calculated with the model parameters in Table 1. Increasing F has a pronounced effect on the increasing selectivity to methane and a decreasing olefin content of the product spectrum. The hydrogen concentration in the liquid bulk increases, which causes an increase of the termination to paraffins relative to olefins and a decrease of the chain growth parameter.

7. Conclusions

A mathematical design model for a large-scale Fischer–Tropsch SBCR is developed. The model takes into account the water gas shift and Fischer–Tropsch reactions as well as individual hydrocarbon product formation rates. Under the operating conditions investigated the FT SBCR is mainly reaction controlled. This is caused by the limited activity of Fe catalysts on the one hand and the large value of the volumetric mass transfer coefficient of the large bubbles due to frequent bubble coalescence and breakup on the other hand. The model predicts the composition of the gaseous and liquid streams of a large-scale bubble column operating in the churn-turbulent regime as a function of the operating parameters. It provides all the data necessary for reliable scale up, process optimization and prediction of the performance of industrial scale FT bubble column reactors.

References

Deckwer, W. -D., Serpeman, Y., Ralek, M., & Schmidt, B. (1982). Modeling the Fischer–Tropsch synthesis in the slurry phase. *Industrial Engineering Chemical Process Design and Development*, *21*, 231–241.

Erkey, C., Rodden, J. B., & Akgerman, A. (1990). A correlation for predicting diffusion coefficients in alkanes. *Canadian Journal of Chemical Engineering*, *68*, 661–665.

Graaf, G. H., Sijtsema, P. J. J. M., Stamhuis, E. J., & Joosten, G. E. H. (1986). Chemical equilibria in methanol synthesis. *Chemical Engineering science*, *41*, 2883–2890.

Krishna, R., De Swart, J. W. A., Ellenberger, J., Martina, G. B., & Maretto, C. (1997). Gas holdup in slurry bubble columns: effect of column diameter and slurry concentrations. *AIChE J.*, *43*, 311–316.

Krishna, R., & Ellenberger, J. (1996). Gas holdup in bubble columns reactors operating in the churnturbulent regime. *AIChE J., 42*, 2627–2634.

Krishna, R., & Maretto, C. (1998). Scale up of a bubble column slurry reactor for Fischer–Tropsch synthesis. *Studies in Surface Science and Catalysis*, *119*, 197–202.

Van der Laan, G.P. (1999). Ph.D. Thesis, University of Groningen, The Netherlands.

Van der Laan, G. P., & Beenackers, A. A. C. M. (1998). α-Olefin readsorption product distribution model for the gas–solid Fischer–Tropsch synthesis. *Studies in Surface Science and Catalysis*, *119*, 179–184.

Letzel, M. H., Schouten, J. C., Krishna, R., & Van den Bleek, C.M. (1999). Gas holdup and mass transfer in bubble column reactors operated at elevated pressure. *Chemical Engineering Science*, *54*, 2237–2246.

Marano, J. J., & Holder, G. D. (1997a). Characterization of Fischer–Tropsch liquids for vapor–liquid equilibria calculations. *Fluid Phase Equilibrium*, *138*, 1–21.

Marano, J. J., & Holder, G. D. (1997b). General equation for correlating the thermophysical properties of n-paraffins, n-olefins, and other homologous series. 2. Asymptotic behavior correlations for PVT properties. *Industrial Engineering and Chemical Research*, *36*, 1895–1907.

Marano, J. J., & Holder, G. D. (1997c). Asymptotic behavior correlations for thermal and transport properties. *Industrial Engineering and Chemical Research*, *36*, 2399–2408.

Mills, P. L., Turner, J. R., Ramachandran, P. A., & Dudukovic, M.P. (1996). In: K.D.P. Nigam, & A. Schumpe, *Three-phase sparged reactors* (Chapter 5). Amsterdam: Gordon & Breach (1996).

Saxena, S. C., Rosen, M., Smith, D. N., & Ruether, J. A. (1986). Mathematical modeling of Fischer–Tropsch slurry bubble column reactors. *Chemical Engineering Communication*, *40*, 97–151.

De Swart, J. W. A., Krishna, R., & Sie, S. T. (1997). Selection, design and scale up of the Fischer–Tropsch reactor. *Studies in Surface Science and Catalysis*, *107*, 213–218.

Vermeer, D. J., & Krishna, R. (1981). Hydrodynamics and mass transfer in bubble columns operating in the churn-turbulent regime. *Industrial Engineering Chemical Process Design and Development*, *20*, 475–482.